

some of their energy, shifting them thus to the X-ray domain. This combined process is called synchrotron self-Compton emission and is a function of the source size: smaller sources have a larger self-Compton component compared to the synchrotron component. Sources for which the luminosity and size are such that the brightness temperature is in excess of  $\sim 10^{12}$  K should emit much more in the X-rays than in the synchrotron branch. This is known as the Compton catastrophe, and is not observed in active galactic nuclei. In quasars, the source size is estimated using the variability timescale of the source, and if the brightness temperature calculated with the infrared or radio flux and variability timescale is in excess of the Compton limit, one can deduce that the true source luminosity is smaller than what can be calculated from the observed flux using an isotropic emission geometry. The simplest anisotropy is that the source is moving relativistically towards the observer, thus boosting the synchrotron flux in the direction of the observer.

In 3C 273, the observations described here imply a brightness temperature well below the Compton limit. However, we have some observations at longer wavelength close to the February infrared maximum, and these observations indicate that the flux continues to rise towards the longer wavelengths, so that, if the spectrum of the March 10

event is similar to the February 25 maximum or if rapid variability also occurred around February 25 (both are probable but neither can be established with our spectral and temporal sampling), then the brightness temperature is in excess of the Compton limit. Further evidence along these lines comes from the mm observations performed this year: Preliminary results (Robson et al., in preparation) indicate very rapid variations and therefore extremely high brightness temperatures, well in excess of the Compton limit. It is therefore possible that the source of the flares is moving at relativistic speeds towards the observer.

The evidence for a brightness temperature in the flares of 3C 273 well in excess of the Compton limit, and thus of relativistic bulk motion of the flare source, is important as it suggests that the emission region is associated with the superluminal jet observed with VLBI (Cohen et al. 1987). This jet is highly structured with new knots appearing at more or less regular intervals and moving away from the source at very high velocities. The flares could then well be the first signs of a new knot appearing in the jet.

The very rapid variations observed during the flare of the bright quasar 3C 273 cast some doubt on the observations of previous flares in this source. It is clear that observations with a less dense temporal sampling would have missed most of the structure we ob-

served and led to quite different conclusions. Also the very structured nature of the flares may be somewhat discouraging for observers, as it indicates that daily observations at least are required to study this type of events. However, this structure also indicates that there is a wealth of information to be obtained on the source geometry, on the acceleration of electrons to relativistic energies and on emission processes. This information will certainly prove important to constrain detailed models of the emission region. Future observations will have to find the relationships between the flaring activity and the other properties of the quasar and try to find what triggers the beginning of a flare, and so maybe help understand the nature of the superluminal jet.

We could obtain a dense spectral and temporal sampling of the 3C 273 flares only with the help and assistance of many rapid reactions to our requests at ESO and in Hawaii.

## References

- Angione R. J. and Smith H. J., 1985, *Astron. J.* **90** (12), 2474.  
 Cohen M. H., Zensus J. A., Biretta J. A., Comoretto G., Kaufmann P. and Abraham Z., 1987, *Astrophys. J.* **315**, L89.  
 Courvoisier T. J.-L., Robson E. I., Blecha A., Bouchet P., Hughes D. H., Krisciunas K. and Schwarz H. E., 1988, *Nature* **335**, 330.

# UM 425: a New Gravitational Lens Candidate

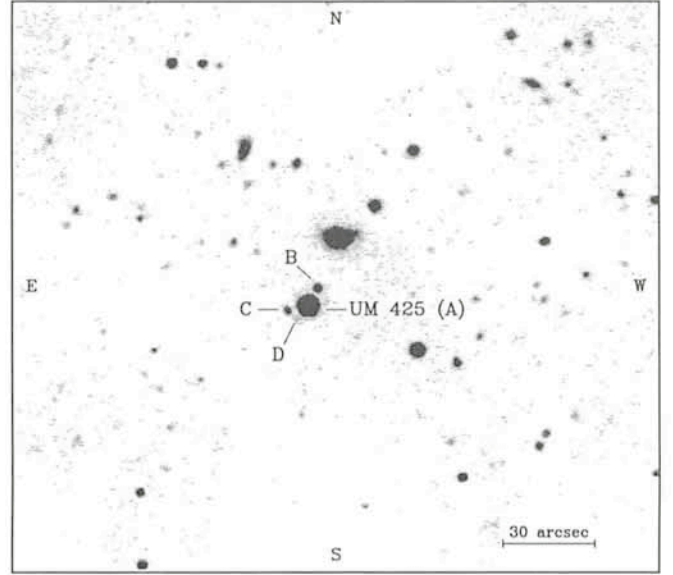
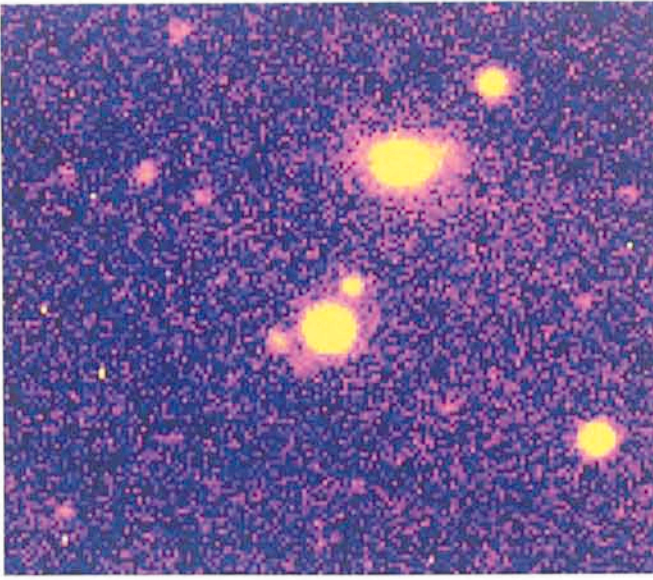
G. MEYLAN, ESO, and S. DJORGOVSKI, CalTech, Pasadena, USA

## I. Introduction

Since the first theoretical discussions more than 50 years ago on the phenomenon of light rays bent by intervening mass in the universe (Eddington 1920, Einstein 1936, Zwicky 1937 a, b), gravitational lensing has steadily grown to become one of the most active fields of research in extragalactic astronomy today. There are numerous theoretical investigations (Refsdal 1964, 1966, Turner et al. 1984, Blandford and Narayan 1986, Blandford and Kochanek 1987 a, b), but the observations of good gravitational lens candidates are still rare. It is only during the last decade that a few quasar systems have been found in reasonable agreement with the gravitational lensing interpretation, viz., 0957+561 (Walsh et al. 1979), 1115+080 (Weymann et al. 1980), 2016+112 (Lawrence et al. 1983),

2237+030 (Huchra et al. 1985), 0142-100 (Surdej et al. 1987), and 1413+117 (Magain et al. 1988). In other possible cases, e.g., 2345+007 (Weedman et al. 1982), and 1635+267 (Djorgovski and Spinrad 1984), there has so far been no detection of lensing galaxies, and thus they should possibly be considered as genuine pairs of interacting quasars, similar to the probable binary quasar PKS 1145-071 (Djorgovski et al. 1987). Recently, so-called giant luminous arcs have been observed in a few clusters of galaxies. They are interpreted as segments of Einstein rings, created because of an almost perfect alignment of the lensing cluster potential well with the lensed background object (Soucail et al. 1988, Lynds and Petrosian 1988). Blandford and Kochanek (1987) provide the most comprehensive and updated review on these subjects.

To improve our knowledge on the phenomenon of gravitational lensing, we are conducting an optical imaging survey for lensed quasars, with a spectroscopic follow-up for the promising cases. The quasar UM 425 = QSO 1120+019 (MacAlpine and Williams 1981) is one of the objects selected as potential lens candidates on the basis of two criteria: a large apparent optical luminosity ( $M_V \leq -28$ ), and a relatively large redshift ( $z \geq 1.5$ ). These simple criteria, chosen to reflect possible gravitational magnification (luminosity) and to provide a large intercept length (redshift), increase the a priori probability that a quasar selected from a magnitude-limited sample is lensed. The efficiency of such simple criteria is demonstrated by the present case, by a few other candidates from our survey which are still awaiting confirmation,



Figures 1a and 1b: Central part (Fig. 1a in false colours and Fig. 1b in grey scale) of an image of the quasar UM 425 (digital stack of V and R frames) obtained with a charge-coupled device (CCD) and the Cerro Tololo Interamerican Observatory (CTIO) 1.5-m telescope, on UT 1987 March 2. The high luminosity quasar is resolved into at least four images. Two quasi-stellar images, the main component A and its brightest companion B, separated by 6.5 arcsec, have  $V = 16.2$  mag and  $V = 20.8$  mag, respectively. The C component ( $V = 21.8$  mag) and the even fainter D component are similar to the numerous nonstellar objects in the field, suggestive of a rich foreground ( $z = 0.6?$ ) cluster of galaxies.

and by the two cases published by the Liège group (Surdej et al. 1987, Magain et al. 1988). More comprehensive results concerning UM 425 are to be published in *Ap. J. Letters*.

## II. Observations and Results

Because of weather conditions, six observing runs, spread over more than 15 months, were necessary in order to unveil completely the interesting character of the QSO UM 425. Our first charge-coupled device (CCD) imaging observations of this object were obtained with the Cerro Tololo Interamerican Observatory (CTIO) 1.5-m telescope, on the night UT 1987 March 2. The conditions were photometric with a seeing FWHM  $\approx 1.7$  arcsec. Exposures of 600 sec in V and 500 sec in R were obtained, with an additional 1000 sec B exposure on UT 1987 March 5. The images were processed using standard techniques. Figure 1a shows, in false (computerized) colours, the digital stack of the V and R frames. Three close faint companions, labelled B, C, and D (in decreasing luminosity) on the grey scale image displayed in Figure 1b, encircle the bright image of the quasar (A). Our preliminary photometry indicated that the companions B and C have similar or identical colours to the brightest image, A. There is a large number of V  $\sim 22$  mag galaxies in the field, suggesting a rich foreground ( $z \sim 0.6?$ ) cluster. Thus, the initial optical imaging data were consistent with gravitational lensing.

Because of the promising character of these images, snapshots were kindly

taken by Dr. R. Perley with the Very Large Array (VLA) radio telescope in September 1987. The system was not detected at 20 cm and 6 cm.

The follow-up spectroscopy, in marginal weather conditions, with the Mt. Palomar 200-inch telescope, on the night UT 1988 March 8, and with the Las Campanas 100-inch telescope, on the night UT 1988 April 7, indicated inconclusively possible similar emission lines in spectra of components A and B, and possibly also C.

The convincing observations were obtained with the ESO Faint Object and Spectrograph Camera (EFOSC) at the ESO 3.6-m telescope, on the 3 nights UT 1988 May 15, 16, and 17. The weather conditions were nonphotometric with a mean value of the seeing FWHM  $\approx 1.4$  arcsec. Several direct imaging exposures were obtained, with 60 sec integration with the B filter (ESO # 552), 45 sec with the V (ESO # 553), and 30 sec in the R (ESO # 554). The data were processed and added using standard techniques. These reasonably good-seeing images suggest that the component C is somewhat diffuse (non-stellar) in appearance.

The separation between the quasar image A and its brightest companion B is:

$$\begin{aligned}\Delta\alpha_{A-B} &= +3.1 \pm 0.1 \text{ arcsec} \\ \Delta\delta_{A-B} &= -5.7 \pm 0.1 \text{ arcsec},\end{aligned}$$

which corresponds to a separation of 6.5 arcsec in the direction  $PA = -29^\circ$ . The separation between the images A and C is:

$$\begin{aligned}\Delta\alpha_{A-C} &= -6.6 \pm 0.1 \text{ arcsec} \\ \Delta\delta_{A-C} &= +1.8 \pm 0.1 \text{ arcsec},\end{aligned}$$

which corresponds to a separation of 6.8 arcsec in the direction  $PA = +105^\circ$ .

The spectrophotometric magnitudes of the QSO (A), 16.5 B mag, 16.2 V mag, and 15.7 R mag, are uncertain by a couple of tenths of a magnitude, because of the poorly determined zero point, which also plagues our direct imaging. The spectrophotometric colours are much better determined, since the zero-point uncertainties cancel: we obtain  $(B-V)_A = 0.33$ , and  $(V-R)_A = 0.49$ , with the uncertainty of a couple of per cent. However, differences between magnitudes in a given bandpass can be accurately determined from our direct imaging. We obtained a relative photometry of the components A, B, and C by using the point-spread function fitting programme for stellar photometry in DAOPHOT. For the components A and B, we obtain:

$$\begin{aligned}\Delta B_{A-B} &= -4.68 \pm 0.15 \\ \Delta V_{A-B} &= -4.61 \pm 0.08 \\ \Delta R_{A-B} &= -4.42 \pm 0.12,\end{aligned}$$

giving 21.2 B mag, 20.8 V mag, and 20.1 R mag for the component B. Using the spectrophotometric colours of the image A as the zero-point, we derive  $(B-V)_B = 0.40$ , and  $(V-R)_B = 0.68$ . The colours of the component B derived from our spectrophotometry are  $(B-V)_B = 0.36$ , and  $(V-R)_B = 0.67$ , uncertain by a few per cent, and thus in excellent agreement. For the components A and C, the differences in magnitudes are:

$$\begin{aligned}\Delta B_{A-C} &= -6.05 \pm 0.25 \\ \Delta V_{A-C} &= -5.56 \pm 0.15 \\ \Delta R_{A-C} &= -5.77 \pm 0.15,\end{aligned}$$

giving 22.6 B mag, 21.8 V mag, and 21.5 R mag, with  $(B-V)_C = 0.8$ , and

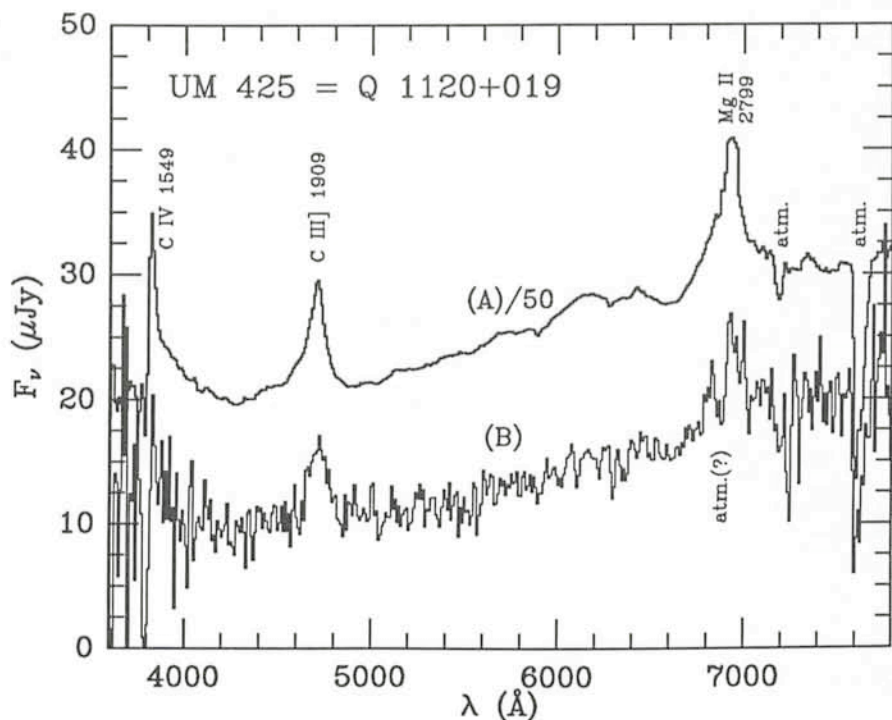


Figure 2: Spectra of the quasar UM 425 (A and B), obtained with the Faint Object and Spectrograph Camera (EFOSC) at the European Southern Observatory (ESO) 3.6-m telescope, on the 3 nights UT 1988 May 15, 16, and 17. Because of the large difference in luminosity between the two components, the spectrum of A is divided by a factor of 50 for display purposes. The spectra are similar in shape and show the same emission lines (C IV 1549, C III] 1909, and Mg II 2799) at the same redshift.

$(V-R)_C = 0.3$ . These colours have uncertainties of about 0.3 mag. The component D, clearly a nonstellar object, is too faint and too close to the bright image A to obtain any reliable measurements. It is about 4–5 arcsec away in the direction  $PA = +150^\circ$ .

Given the measurement errors, these results are consistent with constant colours of the three components, but with two hints: (i) B may be slightly redder than A, perhaps by the presence of an underlying (lensing?) galaxy; (ii) C may be redder than A in  $(B-V)$ , but bluer in  $(V-R)$ , and in view of its apparently nonstellar appearance, it could be (as well as the component D) a member of a faint foreground cluster of galaxies.

During the same 3 nights of May 1988, the spectra of the components A and B were obtained with the B 300 and R 300 grisms of EFOSC. The final usable range in wavelength runs from 3600 to 8000 Å, with a resolution of  $\sim 7$  Å/pixel. The data confirmed immediately that both objects A and B have quasar spectra, with the same emission lines at apparently the same redshift. The resulting spectra for components A and B are displayed in Figure 2. These two spectra are the result of 7 exposures of 1,800 sec in each of the B 300 and R 300 grisms, giving a total of 14 exposures, or 7 hours of integration. The usual strong emission lines are present in both spectra, viz.,

C IV 1549, C III] 1909, and Mg II 2799. The spectra are very similar in the overall shape, and the equivalent widths of

the emission lines are quite comparable: 63.2 and 69.1 Å in the case of C III] 1909 lines, and 74.1 and 70.8 Å in the case of the Mg II 2799 line, for A and B components, respectively.

The comparison between the two spectra is hampered by the strong difference in magnitude between the components, giving very different signal-to-noise ratios: e.g.,  $(S/N)_B \sim 6$  when  $(S/N)_A \sim 350$ . The Mg II line appears to be asymmetric, with a possible absorption in its blue side. However, the comparison of the spectra is made difficult by the presence of the B band, which we can remove only partly. Some absorption feature could also be present in the blue side of the C IV line. Data with a higher S/N ratio are needed before the situation is clarified. Consequently, the redshift of the quasar A was obtained by using only the C III] line, the only “clean” emission line in our spectra, and equals  $z_{A,1909} = 1.465 \pm 0.005$ . From the C IV line, we obtain  $z_{A,1549} = 1.469$ , and from Mg II line,  $z_{A,2799} = 1.476$ .

We looked for a possible difference in redshift between the two spectra (A and B), using the cross-correlation technique. The different measurements were done by varying the limits of the wavelength range used (from  $\sim 4000$  to  $\sim 7200$  Å) and giving mean value of the redshift difference  $\Delta z_{A-B} = (-1.5 \pm 2.0) \times 10^{-3}$ , corresponding to the rest-frame

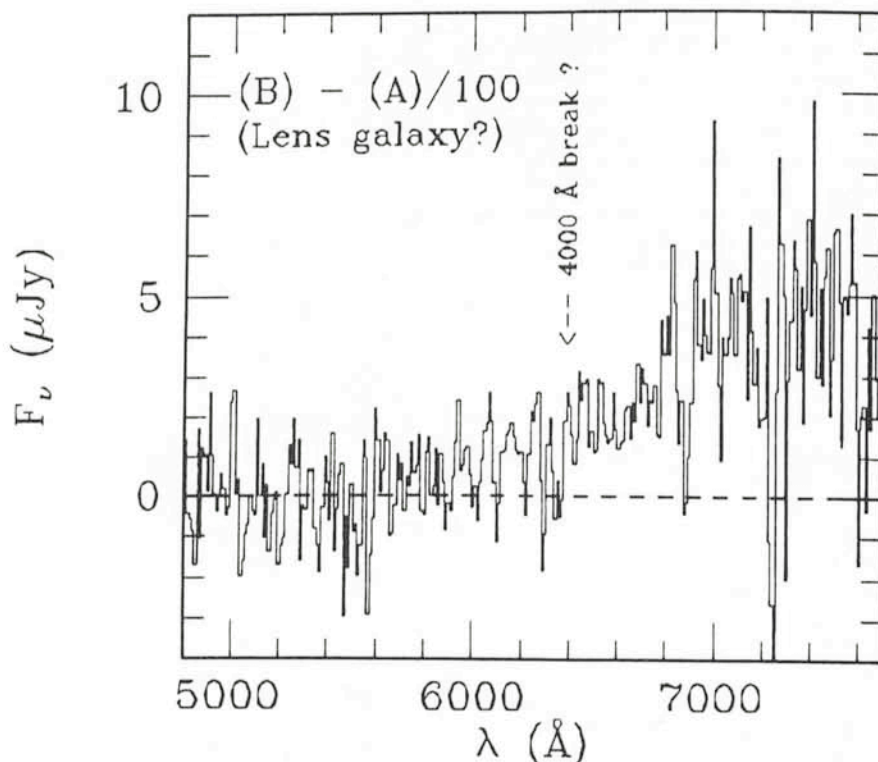


Figure 3: Residual spectrum obtained after dividing the spectrum of the component A by 100 and subtracting it from the spectrum of the component B. Each original spectrum corresponds to 3.5 hours of integration time in each grism. The residual spectrum difference is reminiscent of an early-type galaxy spectrum at a redshift  $z \sim 0.6$ , if the continuum rise at  $\sim 6400$  Å is attributed to the 4000 Å break.

velocity difference  $\Delta v_{A-B}^r = -180 \pm 240 \text{ km s}^{-1}$ , and a median value  $\Delta z_{A-B} = (+1.3 \pm 2.0) \times 10^{-3}$ , or  $\Delta v_{A-B}^r = +160 \pm 240 \text{ km s}^{-1}$ . These very preliminary measurements are then consistent with a zero velocity difference between the components A and B, to within  $\sim 300 \text{ km s}^{-1}$ . Additional data are needed in order to improve on this measurement.

The result of the division of the two spectra (B/A) is fairly constant in the blue part (3600–6400 Å), and a slight but significant increase in the red part (6400–8000 Å), which is equivalent to the slight difference in colour, noted above. It is possible to consider the apparent reddening of the component B as a contribution from a foreground galaxy which could be a part of the gravitational lens itself. We divided the spectrum of the component A by 100 (very close to the flux ratio from the division), and subtracted it from the spectrum of the component B. The resulting spectrum, shown in Figure 3, is reminiscent of an early-type galaxy spectrum at a redshift  $z \sim 0.6$ , if the continuum rise is attributed to the 4000 Å break (see Surdej et al. 1987 for a similar investigation). The rough R magnitude of this component is  $\sim 23 \pm 0.5$  (about 7<sup>m</sup> fainter than A and 2<sup>m</sup> fainter than B), comparable to what is expected of a luminous elliptical galaxy at  $z \approx 0.6$  (Guiderdoni and Rocca-Volmerange 1987). The large number of other faint galaxies in the field is also consistent with the presence of a rich foreground cluster at that redshift. Finally, it is possible that the companion D (and perhaps even C) are other members of this hypothetical lensing cluster along the line of sight to UM 425. The brighter ( $V = 17.8$ ) galaxy just NW from UM 425 is at  $z = 0.1265$ , and probably unrelated to the system.

### III. Conclusion

It is worth mentioning that it is a generic feature of gravitational lensing that the closer the component separation, the greater the similarity of their relative intensities, and vice versa. In the present case, because of the relatively large image separation (6.5 arcsec), a large difference in brightness is expected and observed (almost a factor of 100). Furthermore, in simple geometry model, the lensing galaxy is expected to be closer to the faint image B than to the bright image A. However, in the case of UM 425, the lensing potential is probably fairly complicated, and we postpone any modelling of the system to a future, more comprehensive paper.

The very similar spectra and colours, the presence of a possible lensing galaxy and/or a cluster, and the luminosity and redshift bias used to select the object in the first place, argue in favour of the gravitational lens hypothesis. It is regrettable that the system is not detected in the radio, as the comparison of the optical and radio images can be used as a powerful test for lens candidates (Djorgovski et al. 1987). Further data are needed in order to tighten the measurements presented here, and establish the nature of the components C and D.

It is a pleasure to thank the staff of all observatories involved, and especially H. Pedersen and J. Miranda at ESO, J. Bravo and M. Navarete at CTIO, W. Kunkel and P. Schecter at Las Campanas, and J. Carrasco at Palomar. Many thanks also to R. Perley for obtaining and reducing the VLA snapshots.

### References

- Blandford, R.D., and Narayan, R. 1986, *Astrophys. J.*, **310**, 568.  
 Blandford, R.D., and Kochanek, C.S. 1987,

- in *Dark Matter in the Universe*, Jerusalem Winter School for Theoretical Physics, eds. Bahcall, J., Piran, T., and Weinberg, S. (Singapore: World Scientific), p. 133.  
 Blandford, R.D., and Kochanek, C.S. 1987, *Astrophys. J.*, **321**, 658 and 676.  
 Djorgovski, S., and Spinrad, H. 1984, *Astrophys. J.*, **282**, L1.  
 Djorgovski, S., Perley, R., Meylan, G., and McCarthy, P. 1987, *Astrophys. J.*, **321**, L17.  
 Eddington, A.S. 1920 *Space, time, and Gravitation*, Cambridge: Cambridge University Press.  
 Einstein, A. 1936, *Science*, **84**, 506.  
 Guiderdoni, B., and Rocca-Volmerange, B. 1987, *Astr. Astrophys.*, **186**, 1.  
 Huchra, J., Gorenstein, M., Kent, S., Shapiro, I., and Smith, G. 1985, *Astron. J.*, **90**, 691.  
 Lawrence, C., Schneider, D., Schmidt, M., Bennett, C., Hewitt, J., Burke, B., Turner, E., and Gunn, J. 1983, *Science*, **223**, 46.  
 Lynds, R., and Petrosian, V. 1988, *Astrophys. J.*, in press.  
 MacAlpine, G.M., and Williams, G.A. 1981, *Astrophys. J. Suppl.*, **45**, 113.  
 Magain, P., Surdej, J., Swings, J.-P., Borgeest, U., Kayser, R., Kühr, H., Refsdal, S., and Rémy, M. 1988, *Nature*, **334**, 325.  
 Refsdal, S. 1964, *Mon. Not. R. Astr. Soc.*, **128**, 307.  
 Refsdal, S. 1966, *Mon. Not. R. Astr. Soc.*, **132**, 101.  
 Soucail, G., Mellier, Y., Fort, B., Mathez, G., and Cailloux, M. 1988, *Astr. Astrophys.*, **191**, L19.  
 Surdej, J., Magain, P., Swings, J.-P., Borgeest, U., Courvoisier, T.J.-L., Kayser, R., Kellerman, K.I., Kühr, H., and Refsdal, S. 1987, *Nature*, **329**, 695.  
 Turner, E.L., Ostriker, J.P., and Gott, J.R. III 1984, *Astrophys. J.*, **284**, 1.  
 Walsh, D., Carswell, R.F., and Weymann, R.J. 1979, *Nature*, **279**, 381.  
 Weedman, D.W., Weymann, R.J., Green, R.F., and Heckman, T.M. 1982, *Astrophys. J.*, **255**, L5.  
 Weymann, R.J., Latham, D., Angel, J.R.P., Green, R.F., Liebert, J.W., Turnshek, D.A., Turnshek, D.E., and Tyson, J.A. 1980, *Nature*, **285**, 641.  
 Zwicky, F. 1937 a, b, *Phys. Rev.*, **51**, 290 and 679.

## Binary Nuclei of Planetary Nebulae

A. ACKER, G. JASNIEWICZ, Equipe "Populations Stellaires", Observatoire de Strasbourg, France

### Introduction

About ten planetary nebulae have late-type central stars, which are too cool to ionize the nebula. This implies either the presence of a warmer companion (the true central star), or an unstable central star which was hotter in the past.

These two phenomena – binarity and intrinsic variability –, which are physically very different, may give rise to appar-

ently very similar variations: same behavior for the radial velocity curve and/or for the light curve. In addition, in both cases, spectral peculiarities can be observed, such as stellar emission lines, which can be explained by chromospheric activity of the star or by mass exchange in a close binary system.

The true interpretation is possible only if coordinated observations are conducted.

### Observations

At La Silla we used various tools:  
 – Radial velocity scanner CORAVEL mounted on the Danish 1.5-m telescope (observations taken by Prévot from Marseille);  
 – Differential photometer P7 of the Geneva Observatory mounted on the Swiss 70-cm telescope;  
 – Spectrograph B & C (CCD detector) mounted on the ESO 1.52-m telescope.